



J. Serb. Chem. Soc. 74 (7) 817–831 (2009)
JSCS–3879

Micromechanical and structural properties of nickel coatings electrodeposited on two different substrates

JELENA LAMOVEC^{1**}, VESNA JOVIĆ^{1#}, RADOSLAV ALEKSIĆ²
and VESNA RADOJEVIĆ²

¹*Institute of Chemistry, Technology and Metallurgy – Center of Microelectronic Technologies and Single Crystals, Njegoševa 12, Belgrade and* ²*Faculty of Technology and Metallurgy, University of Belgrade, Karnegijeva 4, Belgrade, Serbia*

(Received 23 December 2008, revised 14 April 2009)

Abstract: Fine-structured nickel coatings were electrodeposited from a sulfamate-based electrolyte onto different substrates: polycrystalline cold-rolled copper and single crystal silicon with (111) orientation. The influence of the substrate layers and chosen plating conditions on the mechanical and structural properties of these composite structures were investigated by Vickers microhardness testing for different loads. Above a certain critical penetration depth, the measured hardness value was not the hardness of the electrodeposited film, but the so-called “composite hardness”, because the substrate also participated in the plastic deformations during the indentation process. Two composite hardness models (Chicot–Lesage and Korsunsky), constructed on different principles, were chosen and applied to the experimental data in order to distinguish film and substrate hardness. The microhardness values of the electrodeposited nickel layers were mainly influenced by the current density. Increasing the current density led to a decrease in grain size, which resulted in higher values of the microhardness.

Keywords: Vickers microhardness; composite hardness; hardness models; nickel electrodeposition; sulfamate-based electrolyte.

INTRODUCTION

One of the areas of microelectromechanical systems (MEMS) is to fabricate small integrated systems containing sensors, actuators, signal conditioning circuits and additional functional devices with physical dimensions ranging from a couple to a few hundred micrometers. These micromechanical parts are fabricated by selected combinations of different materials and technologies and may be represented as composite structures of substrate (bulk) materials and thin

* Corresponding author. E-mail: jejal@nanosys.ihm.bg.ac.rs

Serbian Chemical Society member.

doi: 10.2298/JSC0907817L

films/coatings. Due to this, good mechanical material properties are critical for the integrity of microsystems. Tribology (friction and wear) is an important factor affecting the performance and reliability of MEMS.

Electrodeposition is a promising technology, especially for the realization of different movable structures for MEMS applications. It is important that it is possible to fabricate movable structures consisting of layers with a very low level of internal (residual) stress. This can be achieved with various materials with widely diverse properties, such as composition, crystallographic orientation and grain size. The properties of electrodeposited materials are affected by the processing parameters. Through controlling the grain size and microstructure, metals can be strengthened and hardened with little or no loss of ductility. Electrodeposition is an IC compatible, low-temperature and high rate deposition technology.

Nickel is widely used material for electrodeposition. Conventional, large-grained nickel is expected to deform whereas electrodeposited fine-grain-structured nickel will resist. Electrodeposited nickel has good mechanical properties, such as high yield strength and hardness, which are beneficial in high-aspect-ratio microstructures.

As a guide to the ability of a material to resist deformation, especially for thin films and coatings, the indentation hardness test is commonly used. An evaluation of the hardness of thin films and coatings (for some materials up to 50 μm -thick films) is difficult to realize because the influence of the substrate must be considered. The measured hardness varies continuously with indentation depth, film thickness and the hardness of the film and the substrate. The substrate commences to contribute to the measured hardness at indentation depths of the order of 0.07–0.20 times the coating thickness. Above a certain critical penetration depth, the measured hardness is called composite hardness and includes a component of the substrate hardness.

COMPOSITE HARDNESS MODELS

There is a necessity to obtain the hardness of the coating alone from experimental composite hardness measurements. Several models which operate on a number of different principles exist. The predictive model advanced by Chicot–Lesage and descriptive model by Korsunsky will be examined and applied to different types of composite systems.

The model proposed by Chicot and Lesage (the C–L model) avoids knowledge or choice of any data other than that obtained easily from standard measurements (thickness and apparent hardness).^{1,2} They constructed a model based on the analogy between the variation of the Young modulus of reinforced composites as a function of the volume fraction of particles and the variation of the composite hardness between the hardness of the substrate and that of the film.³

The value of hardness deduced from an indentation test is not constant because hardness is load-dependent. The Meyer law expresses the variation of the size of the indent, d , as a function of the applied load, P . For the particular case of a film-substrate couple, the evolution of the measured diagonal and the applied load can be expressed by a similar relation to that of Meyer:

$$P = a * d^{n^*} \quad (1)$$

The variation part of the hardness number with load is represented by the factor n^* . They then adopted the following expression:

$$f\left(\frac{t}{d}\right) = \left(\frac{t}{d}\right)^m = f \quad \text{where: } m = \frac{1}{n^*} \quad (2)$$

Now the composite hardness can be expressed by the following relation:

$$H_C = (1-f) / \left(1/H_S + f \left(\frac{1}{H_F} - \frac{1}{H_S} \right) \right) + f(H_S + f(H_F - H_S)) \quad (3)$$

The hardness of the film is the positive root of the following equation:

$$AH_F^2 + BH_F + C = 0 \quad (4)$$

with:

$$A = f^2 (f - 1)$$

$$B = (-2f^3 + 2f^2 - 1)H_S + (1-f)H_C$$

$$C = fH_C H_S + f^2 (f - 1)H_S^2$$

The value of m (composite the Meyer index of the composite) is calculated by a linear regression performed on all the experimental points obtained for a given film substrate couple and deduced from the relation:

$$\ln d = m \ln P + b \quad (5)$$

With the value of m known, only the hardness of the films remains to be calculated.

Korsunsky and co-workers^{4,5} advanced a different approach to analyze hardness data for coated materials, employing dimensionless parameters. The model is applicable to either plasticity- or fracture-dominated behavior, with all scales measured relative to the coating thickness. The approach is based on the assumption that the total work-of-indentation during a hardness test is composed of two parts: the plastic work of deformation in the substrate and the deformation and/or fracture energy in the coating. The composite hardness, H_C , according to this model is given by:

$$H_C = H_S + \left[\frac{1}{1 + k' d^2 / t} \right] (H_F - H_S), \quad k' = \frac{k}{49t} \quad (6)$$

where k represents a dimensionless materials parameter related to the composite response mode to indentation, d is the indent diagonal and t is the thickness of the film. It is not possible to compute the film hardness at each indentation diagonal value since the magnitude of k should also be determined simultaneously from the experimental measurements of the composite hardness. This model does not allow the change in the film hardness with the indentation diagonal to be computed from the individual measurements of this property.

EXPERIMENTAL

The materials chosen for the experimental investigation were electrodeposited nanocrystalline Ni on two different substrates: polycrystalline cold-rolled copper and single crystal Si wafers with (111) orientation. The plating base for the silicon wafers were sputtered layers of 100 Å Cr and 800 Å Ni. Electroplating was performed using the direct current galvanostatic mode from a sulfamate bath consisting of 300 g/l Ni(NH₂SO₃)₂ 4H₂O, 30 g/l NiCl₂ 6H₂O, 30 g/l H₃BO₃ and 1.0 g/l saccharine. The pH value and the temperature of the process were maintained at 4.00 and 50 °C, respectively. The current density values were maintained at 10 and 50 mA cm⁻², which resulted in variations in the microstructures and thus in the mechanical properties. The deposition time was determined according to the plating surface and projected thickness of the deposit (2–50 μm).

In order to observe the coating microstructure, a solution of 25 ml water, 25 ml acetic acid and 50 ml nitric acid was used as an etchant. Coating microstructures were characterized by conventional scanning electron microscopy (SEM).

The mechanical properties of the films were characterized using a Vicker's microhardness tester "Leitz, Kleinhartepuffer DURIMET I" using up to 15 loads, ranging from 4.9 down to 0.049 N. Three indentations were made at each load, yielding six measurements of the indentation diagonals, from which the average hardness could be calculated. The indentation was performed at room temperature. The experimental data were fitted with GnuPlot, version 4.0 (<http://www.gnuplot.info/>).

Following the mechanical testing, the samples were prepared for examination by metallographic microscopy (Carl Zeiss microscope "Epival Interphako").

The topographic details were investigated by means of an atomic force microscope (AFM) named "TM Microscopes – Veeco", operating in the non-contact mode.

RESULTS AND DISCUSSION

Surface morphology

The structure of the electrodeposited nickel is related to the plating variables, such as type of electrolyte bath, current density, pH value and temperature.

An SEM image of the surface morphology of an as-plated sample deposited at a current density of 10 mA cm⁻² is shown in Fig. 1. According to the literature, plated structures consist of small substructures, named "colonies", with deep, large crevices between them.⁶ They were defined as series of very fine grains that tend to form groups.

An SEM picture of an etched plated surface under a higher magnification than previous one is shown in Fig. 2, from which very fine substructures can be seen. The size of these structures are of the order of $0.5\text{--}3\ \mu\text{m}$. From this Figure, it is not possible to determine whether the observed structures are grain boundaries or colonies. A colony boundary may be a grain boundary, but a grain boundary is not necessarily defined by a colony boundary, which may contain finer grains.⁶

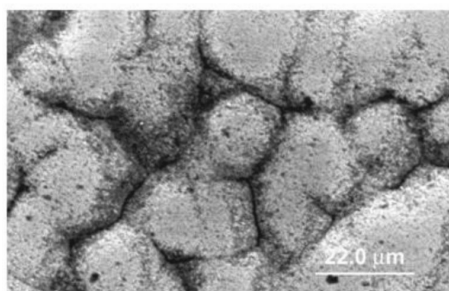


Fig. 1. SEM Image of the as-plated surface morphology that can be seen in samples deposited at a current density of $10\ \text{mA}\cdot\text{cm}^{-2}$. The plated structures consist of small substructures, named “colonies”, and deep, large crevices among them. They were defined as a series of very fine grains that tend to form groups.

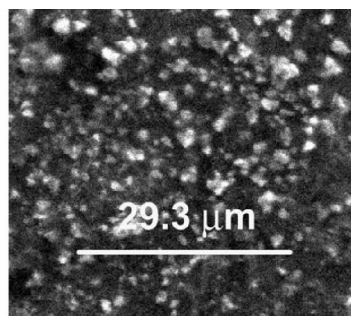


Fig. 2. With increasing depth moving towards the Ni film-substrate interface, the film structures become smaller. The dimensions of these structures are of the order of $0.5\text{--}3\ \mu\text{m}$. A colony boundary may be a grain boundary, but a grain boundary is not necessarily defined by a colony boundary, which may contain finer grains.

From the AFM of the etched surface of a nickel film ($10\ \mu\text{m}$, $50\ \text{mA}\ \text{cm}^{-2}$) shown in Fig. 3, the colonies appear like columnar grains with deep crevices among them.

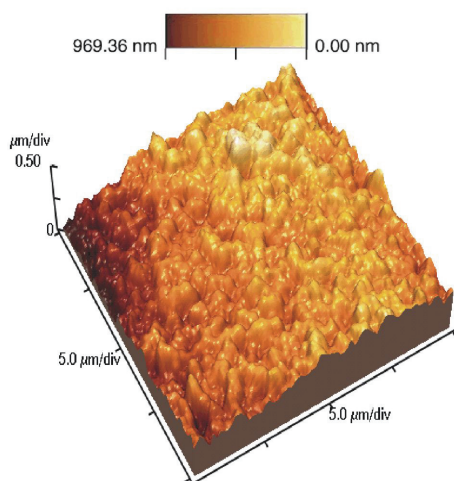


Fig. 3. Topographic AFM image of an electrodeposited Ni film ($10\ \mu\text{m}$, $50\ \text{mA}\ \text{cm}^{-2}$) etched for 60 s showing structures of columnar grains.

Determination of the absolute hardness of the substrates

Tests were performed with a Vickers diamond pyramidal indenter both on uncoated substrates and various coated substrates. Vickers microhardness indentation tests were performed on a Si single crystal substrate in such a way that the indent diagonal was parallel with the prime flat (*i.e.*, the diagonals were parallel to the <110> orientations). It is well known that the mechanical properties of single crystals depend on the crystallographic orientation and this indenter orientation procedure was strictly applied during indentation.⁸

The average values of the impression diagonals, d , were calculated from several independent measurements on every specimen for different applied loads P . The composite hardness, H_C , was calculated using the formulae:

$$H_C = 0.01854Pd^{-2} \quad (7)$$

where 0.01854 is a geometrical factor for the Vickers pyramid.

The classical Meyer Law, Eq. (1), is insufficient for a description of the experimental data but it was found that the proportional specimen resistance (PSR) model is suitable for analyzing the variation of microhardness with load.⁹ According to the PSR model, the indentation test load, P , is related to indentation size, d , as follows:

$$P = a_1d + d^2P_c / d_0^2 \quad (8)$$

In Eq. (8), P is the critical applied test load above which the microhardness becomes load independent and d_0 is the corresponding diagonal length of the indent. A plot of P/d against d will give a straight line, the slope of which gives the value for the calculation of the load independent microhardness.

The P/d values are plotted against d for the two tested substrates: polycrystalline cold-rolled Cu and single-crystalline (111)-oriented Si in Figs. 4a and 4b, respectively. A linear relationship was confirmed for both substrates. The slope gives the value of P/d_0^2 , which, when multiplied by the Vicker's conversion factor, 0.01854 from Eq. (7) gives the value of the load independent microhardness, H_S . These calculated values are given in Fig. 4 for each substrate.

Composite hardness and film hardness

Two different composite systems were investigated: a hard film of electrodeposited nickel on a soft polycrystalline Cu substrate and a soft film of electrodeposited nickel on a hard single crystal substrate of (111)-oriented Si.

Hard film on a soft substrate. The change of the composite hardness, H_C , of the Ni film on Cu substrate system with the relative indentation depth, expressed as indentation depth h through film thickness t , h/t , is shown in Fig. 5. Nickel films with different thicknesses, ranging from 1.2 up to 50 μm , were obtained with two current densities (10 and 50 mA cm^{-2}).

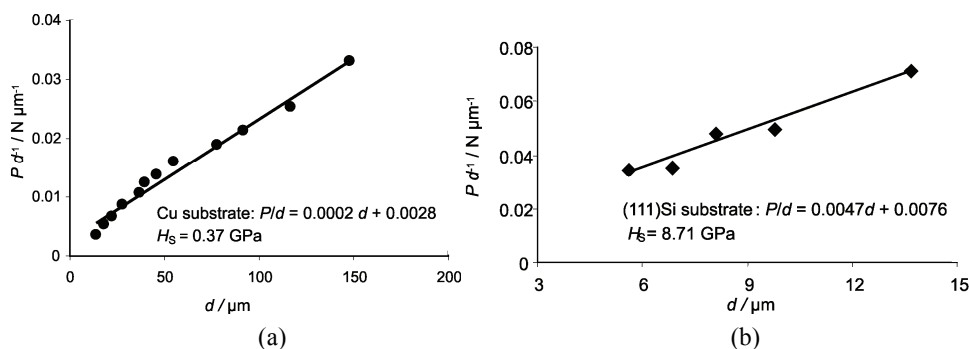


Fig. 4. PSR Plot of applied load through indent diagonal, P/d vs. indent diagonal, d , for a) cold-rolled Cu substrate and b) (111)-oriented single crystal substrate.

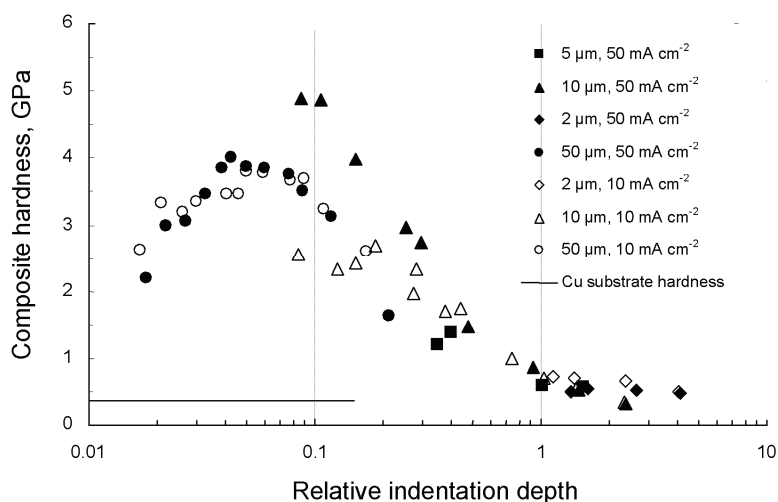


Fig. 5. Variation of the composite hardness, H_C , with the relative indentation depth, h/t , for electrodeposited Ni films on a Cu substrate. Film thickness and deposition current densities are given in the diagram. The thick line represents the hardness of the Cu substrate ($H_S = 0.37$ GPa).

For shallow penetration depths ($h/t \leq 0.10$), it was found that the response was that of the film only. The hardness of the film then increased until a certain relative indentation depth (< 0.1). The films obtained with the higher current density (50 mA cm^{-2}) appeared harder than those deposited with 10 mA cm^{-2} . As the relative indentation depths increased ($h/t > 0.10$), the composite hardness decreased until it attained the substrate hardness H_S , indicated by the solid line in Fig. 5.

The change in the composite hardness H_C , with indentation diagonal d on a cold-rolled Cu substrate is shown in Fig. 6. The experimental data for these systems were fitted with the composite hardness model of Korsunsky, Eq. (6). H_S was taken as 0.37 GPa, according to the experimentally obtained value.

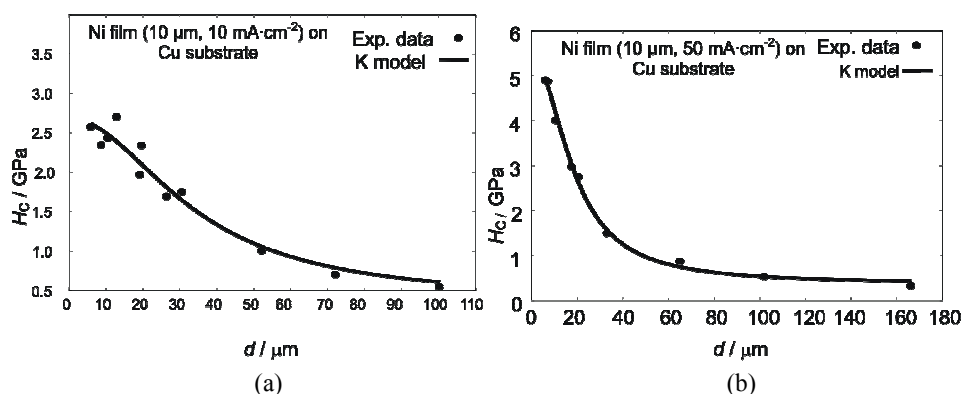


Fig. 6. Experimental values of the composite hardness H_C as a function of the indent diagonal length, d , for two different Ni films on a cold-rolled Cu substrate. The films had the same thickness of 10 μm but were obtained with two different current densities: a) 10 and b) 50 $\text{mA}\cdot\text{cm}^{-2}$. Theoretical description (lines), according to the Korsunsky hardness composite model is given in the diagram.

This model provides a good fit of the experimental data. The indentation tests over the chosen sample covered a large enough range to describe adequately the change in the behavior from near-substrate to film only. In curve-fit data produced from the model validation process for two electrodeposited films are given in Table I.

TABLE I. Values of the fitting results according to the Korsunsky (K) model for the nickel film of 10 μm thickness on a cold-rolled Cu substrate

Quantity	K model	Asymptotic standard error
Electrodeposited Ni film (10 μm , 10 $\text{mA}\cdot\text{cm}^{-2}$) on Cu substrate		
H_F / GPa	2.68	± 0.11 (4.1%)
k^2	0.0087	± 0.0017 (20%)
Electrodeposited Ni film (10 μm , 50 $\text{mA}\cdot\text{cm}^{-2}$) on Cu substrate		
H_F / GPa	5.4	± 0.12 (4.1%)
k^2	0.029	± 0.002 (8.2%)

According to the C–L model, Eq. (3), it is possible to calculate the hardness of the film only from the microhardness testing results (*i.e.*, the diagonal of the indent). For this system, it is valid that the limit of the substrate influence corresponds to $t/d = 1$.^{1,2} Due to this, the model is applicable to film thickness of up to 10 μm for such a particular case. The dependence of the film hardness, H_F , calculated according to the C–L model on the relative indentation depth, h/t , for different film thickness t , different applied loads and different current densities is given in Fig. 7.

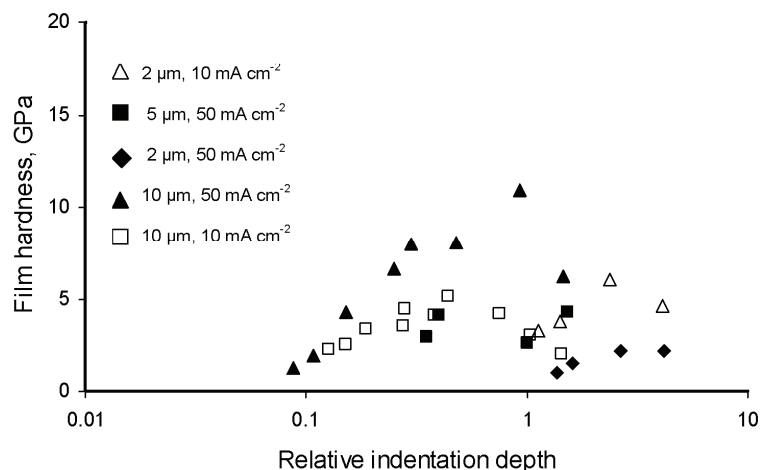


Fig. 7. Calculated film hardness according to the Chicot–Lesage composite hardness model for electrodeposited Ni films of different thicknesses on a Cu substrate. Films of different thicknesses were electrodeposited with two current densities (10 or 50 mA cm⁻²) as indicated in the diagrams.

Soft film on a hard substrate. The change of the composite hardness, H_C , with relative indentation depth, h/t , for Ni films of different thicknesses (2–50 μm) on Si(111) substrates and two values of the current density (10 and 50 mA cm⁻²) is shown in Fig. 8.

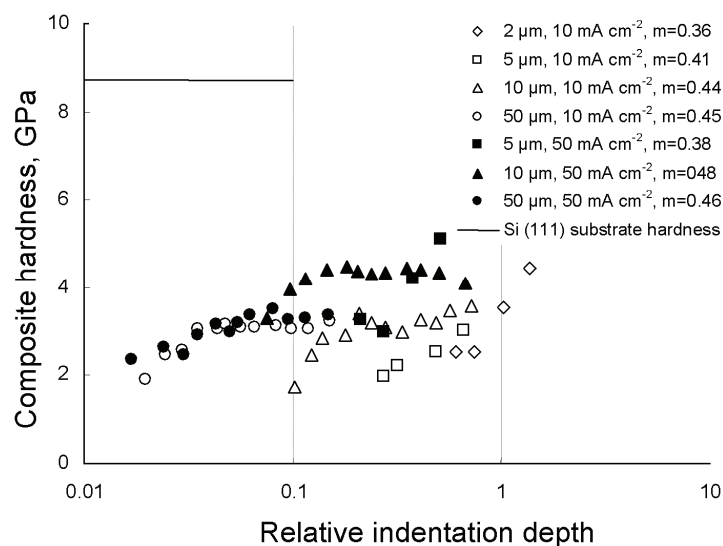


Fig. 8. Variation of composite hardness, H_C , with relative indentation depth, h/t , for electrodeposited Ni films on a (111)-oriented Si substrate. The solid line indicates the hardness of the Si(111) substrate.

It is found that for shallow penetration depths, ($h/t \leq 0.10$), the response was that of the film only. The hardness of the film the increased until a certain relative indentation depth (< 0.10). Films obtained with the higher current density (50 mA cm^{-2}) appear harder than those deposited with 10 mA cm^{-2} .

The change in the composite hardness H_C with indentation diagonal d , for Ni films of $10 \mu\text{m}$ thickness electrochemically deposited with 10 mA cm^{-2} current density on a single crystal Si(111) substrate is shown in Fig. 9. This is the case of a soft coating on a hard substrate. The experimental data for this system was fitted with the composite hardness models of Korsunsky (K-model) and Chicot–Lesage (C–L model). H_S was taken as 8.71 GPa , which is the experimentally determined value for a Si(111) oriented substrate.

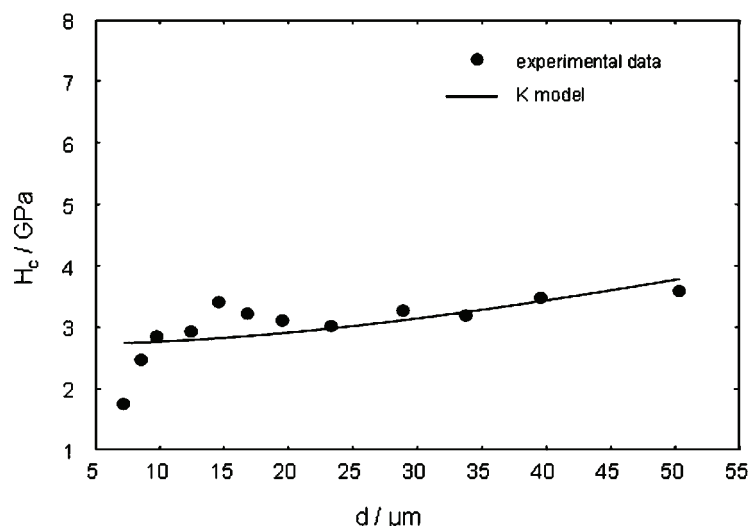


Fig. 9. Experimental values of the composite hardness, H_C , as a function of the indent diagonal length, d , for a $10 \mu\text{m}$ -thick Ni film on a Si(111) substrate. The film was obtained with a current density of 10 mA cm^{-2} . The theoretical description (lines) according to the Korsunsky composite hardness model is indicated in the diagram.

The curve-fit data produced from the K-model validation process for the two electrodeposited films are given in Table II. The standard fitting error given in the same Table indicates that the model does not fit the experimental data for this composite system of a soft coating on a hard substrate well.

TABLE II. Values of the fitting parameters involved in the Korsunsky (K) model for the nickel film of $10 \mu\text{m}$ thickness on a (111)-oriented Si substrate

Quantity	K model	Asymptotic standard error, %
H_F / GPa	2.71	6.27
k^2	0.0008	43.1

The Chicot–Lesage model (C–L) based on the model for reinforced composites can be applied to experimental data even for the thick coatings (50 μm).^{1,2} This model (Eq. (3)) applied to nickel film of different thicknesses, as indicated on the graph, is shown in Fig. 10. The films were obtained with two current densities.

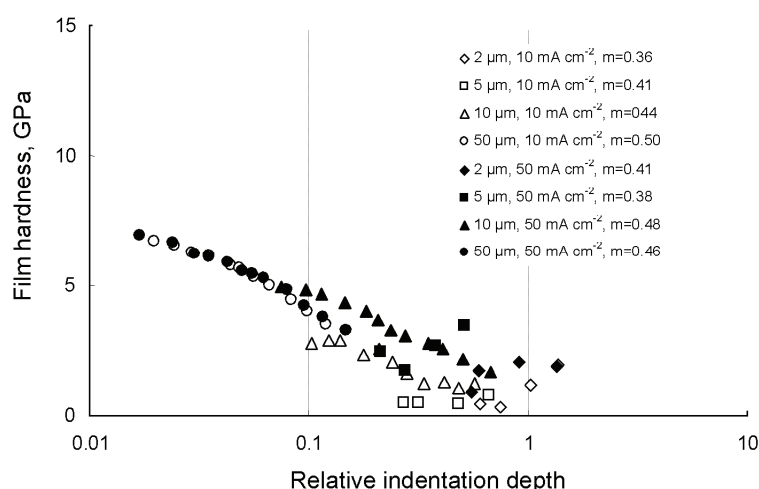


Fig. 10. Variations of the film hardness, H_F , with relative indentation depth, h/t , for the system which consisted of an electrodeposited Ni film on a Si (111) substrate according to the Chicot-Lesage composite hardness model.

As can be seen from Figs. 7 and 10, the values obtained for the film hardness, H_F , were not constant but influenced by the applied load, thickness of the film and current density. The variations should be related to physical phenomena, such as the indentation size effect, cracking in the neighborhood of the indent, the elastic contribution of the substrate for the lowest loads, or the crushing of the film for the highest loads.^{1,2}

Comparison and analysis of the parameter $(t/d)^m$

The Meyer index or work hardening exponent, n^* , describes the variation of hardness with load. The model of Chicot–Lesage gives the parameter m , which is called the composite Meyer index.¹ The composite Meyer index characterizes the manner in which the composite hardness varies with load. Table III shows that the composite Meyer index depended on the composite structure (especially on the substrate type) and had a higher value for the composite Ni film–Cu substrate than for the Ni film–Si(111) composite system.

Figure 11 shows that $(t/d)^m$ is a parameter that can express the difference in tendency of the composite hardness with the indentation load for different composite systems.⁷ For the low loads, the composite hardness tends to that of the

film, and parameter $(t/d)^m$ is independent of the substrate type. With increasing load, the influence of the substrate becomes dominant and parameter $(t/d)^m$ depends mostly on the substrate type. It can be seen that increasing the film thickness above a critical thickness (for these systems, this is 50 μm), leads to insensitivity of this parameter on the substrate type.

TABLE III. Comparison of the composite Meyer index, m , calculated according to the Chicot and Lesage model for different substrates and electrodeposited Ni films obtained with different current densities and with different thicknesses. Ni layer thickness and deposition current density are indicated for every particular layer

Ni films on Cu substrate		Ni films on Si(111) substrate	
$j / \text{mA cm}^{-2}$, $d / \mu\text{m}$	m	$j / \text{mA cm}^{-2}$, $d / \mu\text{m}$	m
10, 2	0.58	10, 2	0.36
10, 10	0.61	10, 10	0.44
10, 50	0.49	10, 50	0.45
50, 2	0.51	50, 2	0.41
50, 5	0.71	50, 5	0.38
50, 10	0.86	50, 10	0.48
50, 50	0.50	50, 50	0.46

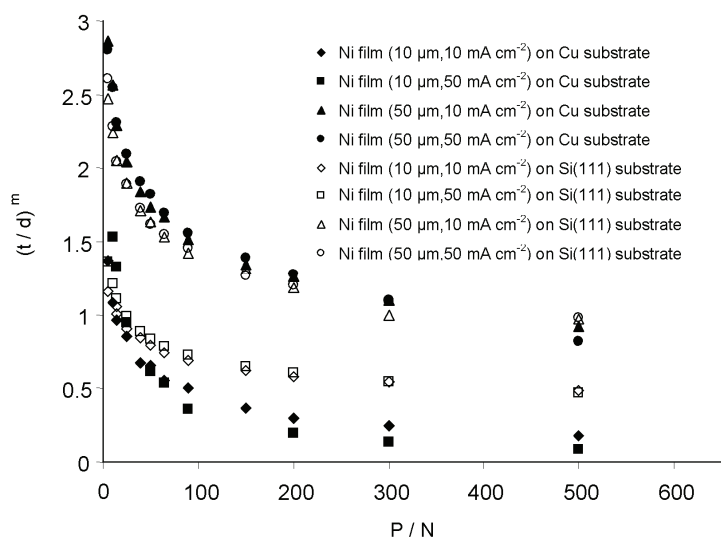


Fig. 11. Comparison of the parameter $(t/d)^m$ with the indentation load, P , for electrodeposited Ni films on a cold-rolled Cu substrate and a single crystal Si(111) substrate. The Ni films, grown with current densities of 10 and 50 mA cm^{-2} , of different thicknesses of 10 and 50 μm .

Hardness and yield strength of fine-grained nickel

The mode of deformation under the indenter described by Tabor follows the results of the slip line field theory for a rigid-plastic material.¹⁰ In this case, it was found that the hardness is related to the yield strength, Y , by:

$$H/Y = 3 \quad (9)$$

It was found that the samples deposited with a current density above 10 mA cm^{-2} obeyed the Hall–Petch relationship. The Hall–Petch plot of yield strength vs. grain size for nickel is shown in Fig. 12 from three studies with an experimental procedure similar to that employed in this study (the different symbols indicate different studies).¹¹

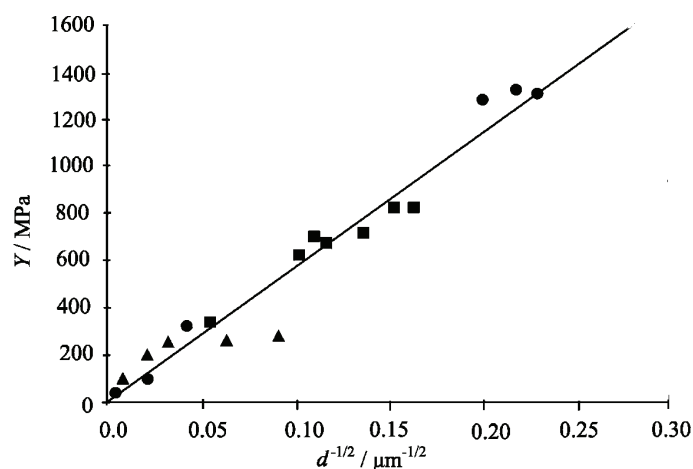


Fig. 12. Yield strength vs. grain size for nickel.

With the results of the film hardness fitted according to the Korsunsky model (Tables I and II), the values of the yield strength were calculated. For the $10\text{-}\mu\text{m}$ Ni films on Cu and (111) Si substrates deposited with a current density of 10 mA cm^{-2} , the yield strengths were 0.893 and 0.903 GPa, respectively (the film microstructure is shown in Figs. 2 and 3). These values of yield strength belong to nanocrystalline nickel with an average grain size of $\approx 30 \text{ nm}$.¹¹

CONCLUSIONS

In order to analyze the hardness of different composite systems, nickel films were electrodeposited on a soft substrate of polycrystalline cold-rolled copper and a hard substrate of single crystal silicon with (111) orientation.

A microstructure of columnar grains, called colonies, with a grain size of the order of $0.5\text{--}3 \mu\text{m}$ was observed.

It was shown that the tendency of the composite hardness primary depends on the type of the composite system, *i.e.*, the differences in the mechanical properties of the film and substrate: the hardness of the substrate, the hardness of the film, their relative difference and, especially, the thickness of the film.

A nickel film on a Cu substrate represents a composite system of a hard film on a soft substrate. The Korsunsky and Chicot–Lesage composite models were

applied to the experimental data for films of up to 10 μm thickness. The Korsunsky model gave a good fit of the results for this type of system. The quality of the fits relied on obtaining experimental hardness data over a wide range of h/t values and almost always this will have to include nano-indentation data. The C–L model was also applicable to this system but there is a necessity for more experiments to be performed and the results of the application verified for this composite system.

Nickel films on a Si(111) substrate can be considered as a soft film on a hard substrate. Korsunsky composite hardness model (K-model) did not fit the experimental data for this composite system well. The Chicot–Lesage model (C–L model), based on the model for reinforced composites, can be applied to the experimental data, even for thick coatings (50 μm). The Chicot–Lesage model was chosen for the system Ni film–Si substrate for all specimens and the film hardness was calculated for each indentation diagonal.

The values obtained for the film hardness, H_F , were influenced by the applied load. In case of the Ni film on Cu substrate system, the film hardness lines exhibited a change of slope, but in case of the Ni film on Si substrate system, the film hardness lines had a descending character. According to Chicot and Lesage explanation, the variations should be related to physical phenomena, such as the indentation size effect, cracking in the neighborhood of the indent, the elastic contribution of the substrate for the lowest loads or the crushing of the film for the highest loads.

The composite Meyer index, m , characterizes the way in which the composite hardness varies with load. When the composite hardness tends to that of the film (for low loads), the parameter $(t/d)^m$ is almost independent of the substrate type. With increasing load, the influence of the substrate became dominant and the parameter $(t/d)^m$ depended mostly on the type of substrate. In addition, with increasing thickness of the film, the influence of the substrate increased for both composite systems. There are not sufficient experimental results concerning the parameter $(t/d)^m$ yet, but it is thought that it deserves more attention in hardness investigations of composite system.

Acknowledgments. This work was performed within the frame of the projects “Micro and Nanosystems Technologies, Structures and Sensors” and “Designing of nanocrystalline magnetic materials of (Nd, Pr)FeB type and smart magnetic materials components”, supported by grants from the Ministry of Science and Technological Development of the Republic of Serbia, Grant No. TR-6151 B and 142035 B, respectively.

ИЗВОД

МИКРОМЕХАНИЧКА И СТРУКТУРНА СВОЈСТВА ЕЛЕКТРОДЕПОНОВАНИХ ПРЕВЛАКА НИКЛА НА РАЗЛИЧИТИМ СУПСТРАТИМА

ЈЕЛЕНА ЛАМОВЕЦ¹, ВЕСНА ЈОВИЋ¹, РАДОСЛАВ АЛЕКСИЋ² и ВЕСНА РАДОЈЕВИЋ²¹Институт за хемију, технологију и металургију – Центар за микроелектронске технологије и монокристале, Њеђошева 12, Београд и ²Технолошко–металуршки факултет, Карнегијева 4, Београд

Ситнозрне превлаке никла су електродепоноване из сулфатног купатила на различитим супстратима: хладно-ваљаном поликристалном бакру и монокристалном силицијуму (111) оријентације. Утицај супстрата и одабраних параметара електродепозиције на механичка и структурна својства ових композитних структура испитиван је тестовима микротврдоће по Vickers-у при различитим оптерећењима. Изнад критичне дубине утискивања, измерена вредност тврдоће није тврдоћа електродепонованог филма, већ такозвана «композитна микротврдоћа», јер супстрат учествује у пластичној деформацији током процеса утискивања. Одабрана су два модела композитне тврдоће базирана на различитим принципима (модел Chicot–Lesage и Korsunsky) и примењена на експерименталне резултате у циљу израчунавања тврдоће филма. Вредности микротврдоће електродепонованих превлака никла зависе од вредности густине струје. Повећање густине струје води смањењу величине зрна и повећању вредности микротврдоће.

(Примљено 23. децембра 2008, ревидирано 14. априла 2009)

REFERENCES

1. J. Lesage, D. Chicot, *Surf. Coat. Technol.* **200** (2005) 886
2. J. Lesage, A. Pertuz, E. S. Puchi-Cabrera, D. Chicot, *Thin Solid Films* **497** (2006) 232
3. W. D. Callister Jr., *Fundamentals of Materials Science and Engineering, An interactive E-text*, 5th ed., Wiley, New York, 2001, p. S-166
4. A. M. Korsunsky, M. R. McGurk, S. J. Bull, T. F. Page, *Surf. Coat. Technol.* **99** (1998) 171
5. J. R. Tuck, A. M. Korsunsky, D. G. Bhat, S. J. Bull, *Surf. Coat. Technol.* **137** (2001) 217
6. S. W. Banovic, K. Barmak, A. R. Marder, *J. Mater. Sci.* **33** (1998) 639
7. J. Lamovec, V. Jović, D. Randjelović, R. Aleksić, V. Radojević, *Thin Solid Films* **516** (2008) 8646
8. M. Tanaka, K. Higashida, H. Nakashima, H. Takagi and M. Fujiwara, *Int. J. Fract.* **139** (2006) 383
9. H. Li, R. C. Bradt, *Mater. Sci. Eng. A* **142** (1991) 51
10. D. Tabor, *The Hardness of Metals*, Clarendon, London, 1951, p. 107
11. J. Guidry, *M.Sc. Thesis*, Louisiana State University, Baton Rouge, LA, 2002, p. 14.